

A precise determination of the charm quark's mass in quenched QCD



Juri Rolf^a and Stefan Sint^{b,c}

- ^a Institut für Physik, Humboldt-Universität zu Berlin, Invalidenstr. 110, D-10115 Berlin, Germany
- ^b CERN, Theory Division, CH-1211 Geneva 23, Switzerland
- ^c Departamento de Física Teórica, Universidad Autónoma de Madrid, 28049 Cantoblanco (Madrid), Spain

Abstract

We present a lattice determination of the charm quark's mass, using the mass of the D_s meson as experimental input. All errors are under control with the exception of the quenched approximation. Setting the scale with $F_K = 160$ MeV, our final result for the renormalization group invariant (RGI) quark mass is $M_c = 1.654(45)$ GeV, which translates to $\overline{m}_c^{\overline{\text{MS}}}(\overline{m}_c) = 1.301(34)$ GeV for the running mass in the $\overline{\text{MS}}$ scheme. A 6 percent increase of the RGI quark mass is observed when the scale is set by the nucleon mass. This is a typical quenched scale ambiguity, which is reduced to about 3 percent for $\overline{m}_c^{\overline{\text{MS}}}(\overline{m}_c)$, and to 4 percent for the mass ratio M_c/M_s . In contrast, the mass splitting $m_{D_s^*} - m_{D_s}$ changes from 117(11) MeV to 94(11) MeV, which is significantly smaller than the experimental value of 144 MeV.

1 Introduction

The charm quark mass is among the fundamental parameters of the Standard Model, and its determination from experimental data is of general interest. In practice it is important to improve on the current precision: the Particle Data Group in its latest edition [1] gives the range

$$1.0 \leq \overline{m}_c^{\overline{\text{MS}}}(\overline{m}_c) \leq 1.4 \text{ GeV}, \quad (1.1)$$

thereby increasing the previously quoted uncertainty [2] by a factor two. The relatively large uncertainty in the charm quark mass has been identified as the dominant error in estimates of the fine structure constant at high energies [3], and in phenomenological estimates of certain B -decay rates [4,5].

A determination of quark masses from experiment is necessarily indirect, as quarks are not observed as free particles. To establish the connection one needs control over the strong interactions at the non-perturbative level. We distinguish two classes of approaches: using some variant of the sum rule technique, one relies on perturbation theory and assumptions such as quark-hadron duality, which allow to connect to quantities derived from experiment [6–10]. While the quoted error especially in [7] is rather small, it seems fair to say that a reliable assessment of the systematic errors is difficult and may not always be possible.

The lattice approach, on the other hand, is non-perturbative in nature and allows to directly compute hadronic observables at fixed lattice spacing and bare quark masses. One may then determine the bare quark masses for which the experimental input is matched. In order to take the continuum limit one must substitute bare by renormalized masses, which are kept fixed as the lattice spacing is varied. It should be emphasized that consistency requires the renormalization procedure to be non-perturbative, too. In recent years there has been significant progress in non-perturbative renormalization techniques [11]. This has led to the determination of the Λ -parameter and the strange quark mass from low-energy hadronic observables, with no uncontrolled systematic errors apart from the quenched approximation [12,13].

In this paper we present a lattice computation of the charm quark mass, where we use the same techniques as for the strange quark mass [13]. In particular we take over the results for the non-perturbative quark mass renormalization of ref. [12], as the renormalization constant is quark mass and hence flavour independent. In addition, all counterterms which are needed to remove the leading lattice artefacts in renormalized quark masses have been determined non-perturbatively in the relevant range of parameters [14,15]. This is an important ingredient, as the charm quark mass is not very small compared to the inverse lattice spacing, so that cutoff effects can be large. Nevertheless, as will be demonstrated below, controlled continuum extrapolations appear to be possible once the leading $O(a)$ artefacts have been cancelled. For this reason our final result for the charm quark mass is much more precise than previous lattice estimates [16–20]. In particular, the dominant

remaining uncertainty stems from the use of the quenched approximation, and further progress will require the inclusion of sea quark effects.

The paper is organized as follows: In section 2 we explain our general strategy and the assumptions made. We then describe the technical framework of our calculation and collect the formulae needed for the quark mass renormalization and $O(a)$ improvement (sect.3). Section 4 contains some details of the numerical simulations and a discussion of systematic errors. Continuum extrapolations and results for the charm quark mass, the charm to strange quark mass ratio and the hyperfine splitting of D mesons are discussed in sect. 5, and we conclude in sect. 6.

2 Strategy

2.1 Experimental input and basic assumptions

It is generally assumed that the experimentally observed light hadron spectrum can be accounted for by considering the physics of strong and electromagnetic interactions between up, down, strange and charm quarks. Furthermore, due to the smallness of the fine structure constant, electromagnetic effects are likely to be small. Experimental results for the light hadron spectrum can thus directly be compared to results of a QCD calculation, possibly after a small correction for electromagnetic effects.

Numerical simulations of lattice QCD offer the possibility to compute the hadronic spectrum with an accuracy of typically a few per cent. One may then turn the tables and use the precise experimental data to determine the free parameters of QCD, i.e. the gauge coupling and the quark masses. For instance, assuming isospin symmetry, $M_u = M_d$, the four remaining parameters can be determined by matching the kaon's decay constant and mass,

$$F_K = 160 \text{ MeV}, \quad m_K = 495 \text{ MeV}, \quad (2.2)$$

the mass of the D_s meson,

$$m_{D_s} = 1969 \text{ MeV}, \quad (2.3)$$

and by taking the quark mass ratio,

$$M_s/\hat{M} = 24.4 \pm 1.5, \quad \hat{M} = \frac{1}{2}(M_u + M_d), \quad (2.4)$$

as determined in Chiral Perturbation Theory [21]. This latter input might be traded e.g. for the pion mass. However, lattice simulations are typically carried out for quarks not very much lighter than the strange quark, so that a chiral extrapolation becomes necessary. As the ansatz for such an extrapolation is usually guided by chiral perturbation theory, the input of the pion mass is in practice not very different from the direct use of eq. (2.4). A similar problem occurs if one attempts to determine the kaon mass and its decay constant at the physical values of the quark masses. Chiral perturbation theory

predicts a very weak dependence upon the difference of the valence quark masses [22,23], and this has been verified numerically to some extent [13]. In practice one then computes with mass degenerate quarks the sum of which matches the sum of the physical light and strange quark masses. Once again, one relies on the assumption that chiral perturbation theory provides a reliable description of the quark mass dependence beyond the range actually covered by the simulations.

2.2 Electromagnetic effects

Electromagnetic effects on hadronic observables involving up, down and strange quarks can be computed in Chiral Perturbation Theory. For instance, the result $m_K = 495 \text{ MeV}$ (2.2) is the (isospin averaged) experimental result after a subtraction of an estimate for the electromagnetic mass shift [13].

For the charm quark mass determination we would like to estimate electromagnetic effects on D -mesons masses, where standard Chiral Perturbation Theory does not apply¹. We propose a phenomenological estimate and shall assume that all pseudoscalar D meson masses can be parameterized in the form

$$m_{\text{PS}} = AM_{\text{light}} + Bq + C, \quad (2.5)$$

where M_{light} is the light valence quark mass and q distinguishes electrically charged ($q = 1$) and neutral ($q = 0$) mesons. Note that a linear dependence on the light valence quark mass is indeed observed in lattice simulations, at least for some range of light valence quark masses [26]. Using this ansatz, we first note that C cancels in the mass differences,

$$m_{D_s^\pm} - m_{D^\pm} = A(M_s - M_d), \quad (2.6)$$

$$m_{D^\pm} - m_{D^0} = A(M_d - M_u) + B. \quad (2.7)$$

We may then eliminate A and solve for the electromagnetic mass shift B ,

$$B = m_{D^\pm} - m_{D^0} - \frac{M_d - M_u}{M_s - M_d} (m_{D_s^\pm} - m_{D^\pm}). \quad (2.8)$$

Taking the mass ratio from Chiral Perturbation Theory [21],

$$\frac{M_d - M_u}{M_s - M_d} = (40.3 \pm 3.2)^{-1}, \quad (2.9)$$

and the experimental data for the mass splittings [2],

$$m_{D_s^\pm} - m_{D^\pm} = 99.2 \pm 0.5 \text{ MeV}, \quad m_{D^\pm} - m_{D^0} = 4.79 \pm 0.10 \text{ MeV}, \quad (2.10)$$

¹see, however, refs. [24,25] for an extension of Chiral Perturbation Theory to mesons containing a heavy quark.

we arrive at the estimate

$$B \approx 2.3 \text{ MeV}. \quad (2.11)$$

Similar considerations can be made for the vector mesons, where this effect is even smaller, and we conclude that electromagnetic effects cause D -meson mass shifts of a few MeV at most. This is below the accuracy currently reached by lattice computations, so that we will neglect electromagnetic effects in the following.

Although there is little doubt that electromagnetic mass shifts are indeed negligible we mention that this could also be checked explicitly, by including an additional U(1) gauge field in the numerical simulations [27].

2.3 Quenched results for the $\Lambda_{\overline{\text{MS}}}$ and M_s

In the quenched approximation the programme outlined above has already been completed except for the charm quark mass, which is the topic of this work. Instead of quoting the value of a running coupling in some renormalization scheme at a reference scale, it is customary to quote the Λ parameter in the $\overline{\text{MS}}$ scheme², viz. [12]

$$\Lambda_{\overline{\text{MS}}}^{(0)} = 238(19) \text{ MeV}. \quad (2.12)$$

Furthermore, the result for the sum of the renormalization group invariant average light and strange quark mass is [13]

$$\hat{M} + M_s = 143(5) \text{ MeV}. \quad (2.13)$$

Using the quark mass ratio (2.4), the latter result translates to

$$M_s = 138(6) \text{ MeV} \quad \Rightarrow \quad \overline{m}_s^{\overline{\text{MS}}}(2 \text{ GeV}) = 97(4) \text{ MeV}, \quad (2.14)$$

for the running mass in the $\overline{\text{MS}}$ scheme of dimensional regularization at the scale 2 GeV. It should be emphasized that these results have been obtained in the continuum limit, by carefully disentangling renormalization and cutoff effects. Thus, the only uncontrolled error arises from the use of the quenched approximation.

2.4 The scale r_0 and the quenched scale ambiguity

The attempt to describe the real world with data obtained within the quenched approximation is bound to fail at some point. In particular, the attribution of physical units to quenched results is ambiguous. To avoid this ambiguity we will quote results in units of

² Note that $\Lambda_{\overline{\text{MS}}}$ can be defined beyond perturbation theory, owing to the fact that the *exact* relation between Λ -parameters of different schemes is determined by the one-loop perturbative relation between the respective couplings. Hence, $\Lambda_{\overline{\text{MS}}}$ can be defined indirectly, by referring to the Λ -parameter of a non-perturbatively defined renormalization scheme.

the low-energy scale r_0 , which is derived from the force between static color sources [28]. This has mostly technical advantages: first, r_0/a has been determined very precisely over a wide range of cutoff values [29–31], so that scaling studies are naturally carried out using this scale. Second, in the absence of dynamical quarks, r_0 is only affected by cutoff effects of order a^2 [31]. The relation to other hadronic scales in the quenched approximation is known [13],

$$r_0 F_K = 0.415(9), \quad r_0 m_N \approx 2.6. \quad (2.15)$$

This illustrates the inconsistency of the quenched approximation, as the quenched result for F_K/m_N differs by 10 per cent from its experimental value. This can be viewed as a scale ambiguity: setting the scale with $F_K = 160$ MeV is roughly equivalent to the choice $r_0 = 0.5$ fm, while $m_N = 938$ MeV corresponds to $r_0 = 0.55$ fm. We will later investigate the effect of this “quenched scale ambiguity”, in order to get a first idea of the size of typical quenching errors.

The results in the previous subsection have been obtained using $r_0 = 0.5$ fm. In units of r_0 we have

$$r_0 \Lambda_{\overline{\text{MS}}}^{(0)} = 0.602(48), \quad r_0 M_s = 0.348(13). \quad (2.16)$$

2.5 Strategy to compute the charm quark’s mass

At fixed cutoff, standard lattice QCD techniques allow to compute meson masses for given bare mass parameters of the meson’s valence quarks. As for the strange quark mass, the results of [13] allow to set its bare mass parameter without further tuning. To determine the bare charm quark mass it thus remains to measure pseudoscalar meson masses for several bare mass parameters, and to interpolate the meson masses versus the bare charm quark mass to the physical point where

$$m_{D_s} = 1969 \text{ MeV} \quad \Rightarrow \quad r_0 m_{D_s} = 4.99. \quad (2.17)$$

Then, using known renormalization factors, one may obtain the renormalization group invariant charm quark mass, M_c , in units of r_0 and at the given value of the cutoff a^{-1} . Repeating the procedure for smaller lattice spacings a , one may eventually extrapolate to the continuum. Additional control of this extrapolation may be obtained by considering alternative definitions of $r_0 M_c$, with different cutoff effects but the same continuum limit.

In the following two sections we describe in some detail the technical setup to achieve this goal. The reader not so much interested in the technicalities may directly go to sect. 5, where the continuum extrapolations and final results are discussed.

3 The technical framework

For the practical implementation of the programme we use the framework of $O(a)$ improved lattice QCD as described in ref.[32]. For unexplained notation we refer to this paper.

3.1 SF correlation functions

In order to extract hadron masses we use correlation functions derived from the QCD Schrödinger functional (SF) [33,34]. Hence, QCD is considered on a space-time manifold which is a hyper-cylinder of volume $L^3 \times T$, with the quantum fields satisfying periodic boundary conditions in space, and Dirichlet boundary conditions at Euclidean times $x_0 = 0$ and $x_0 = T$. The technical advantages for the computation of hadron properties have been demonstrated in [35]. One of the main points is the possibility to define quark and antiquark boundary states ζ and $\bar{\zeta}$, which only transform under spatially constant gauge transformations. Boundary sources with quantum numbers of mesons are therefore gauge invariant even if quark and antiquark fields are localized at different points in space.

For the study of pseudoscalar and vector mesons, we define the axial current and density,

$$A_\mu(x) = \bar{\psi}_i(x)\gamma_\mu\gamma_5\psi_j(x), \quad P(x) = \bar{\psi}_i(x)\gamma_5\psi_j(x), \quad (3.18)$$

and the local vector current,

$$V_\mu(x) = \bar{\psi}_i(x)\gamma_\mu\psi_j(x), \quad (3.19)$$

with flavour indices $i \neq j$. The correlation functions

$$f_A(x_0) = -\frac{1}{2}a^6 \sum_{\mathbf{y}, \mathbf{z}} \langle \bar{\zeta}_j(\mathbf{y})\gamma_5\zeta_i(\mathbf{z})\mathbf{A}_0(\mathbf{x}) \rangle, \quad (3.20)$$

$$f_P(x_0) = -\frac{1}{2}a^6 \sum_{\mathbf{y}, \mathbf{z}} \langle \bar{\zeta}_j(\mathbf{y})\gamma_5\zeta_i(\mathbf{z})\mathbf{P}(\mathbf{x}) \rangle, \quad (3.21)$$

$$k_V(x_0) = -\frac{1}{6}a^6 \sum_{\mathbf{y}, \mathbf{z}} \langle \bar{\zeta}_j(\mathbf{y})\gamma_{\mathbf{k}}\zeta_i(\mathbf{z})\mathbf{V}_{\mathbf{k}}(\mathbf{x}) \rangle, \quad (3.22)$$

are then used to compute pseudoscalar and vector meson masses with valence quark flavours i and j . The notation and technology has been described in detail in ref. [35]. One studies the effective masses

$$am_{\text{eff}}(x_0 + \frac{1}{2}a) = \ln \{f(x_0)/f(x_0 + a)\}, \quad (3.23)$$

where $f(x_0)$ stands for one of the above correlation functions. For large time distances from the boundaries, i.e. large x_0 and $T - x_0$, one expects the ground state of a given channel to dominate the correlation function, which manifests itself in a plateau for the effective mass versus x_0 .

3.2 Definition of renormalized quark masses

The renormalization of quark masses for Wilson type quarks is complicated by the fact that all axial symmetries are explicitly broken by the regularization. As a consequence,

quark mass renormalization is both additive and multiplicative, the axial current requires a scale-independent renormalization, and axial Ward identities, such as the PCAC relation are violated by cutoff effects. There are various ways to define renormalized quark masses, which are equivalent in the continuum limit, but may differ at finite lattice spacing. This will later be used to achieve a better control of the continuum extrapolations.

We start with the definition of a bare current quark mass using the PCAC relation,

$$m_{ij} = \frac{\tilde{\partial}_0 f_A(x_0)}{2f_P(x_0)}, \quad (3.24)$$

where $\tilde{\partial}_\mu = \frac{1}{2}(\partial_\mu + \partial_\mu^*)$ denotes the symmetric lattice derivative in μ -direction. From the bare quark mass m_{ij} we obtain the sum of the renormalized valence quark masses through multiplicative renormalization of the axial current and density in (3.24), viz.

$$m_{R,i} + m_{R,j} = 2Z_A Z_P^{-1} m_{ij}. \quad (3.25)$$

A single quark mass is obtained if the quark flavours i and j are mass degenerate,

$$m_{R,i} = Z_A Z_P^{-1} m_i. \quad (3.26)$$

Another starting point is provided by the hopping parameter in the Wilson quark action. One defines a bare subtracted quark mass,

$$m_{q,i} = \frac{1}{2}(\kappa_i^{-1} - \kappa_{\text{critical}}^{-1}), \quad (3.27)$$

where κ_{critical} is the value of κ at which chiral symmetry is restored. This subtracted bare quark mass is then multiplicatively renormalized,

$$m_{R,i} = Z_m m_{q,i}. \quad (3.28)$$

In what follows, we will always refer to the same renormalization scheme for the quark mass. This is achieved by first defining the renormalized axial current and density, and by setting

$$Z_m = Z Z_A / Z_P, \quad (3.29)$$

where Z is the scale independent ratio between the bare quark masses,

$$m_i = Z m_{q,i}. \quad (3.30)$$

Furthermore, we restrict attention to quark mass independent renormalization schemes. The SF scheme of ref. [36] has this property, and it has the additional virtue of being defined beyond perturbation theory. Its relation to the renormalization group invariant (RGI) quark mass,

$$M_i = \lim_{\mu \rightarrow \infty} \bar{m}_i(\mu) [2b_0 \bar{g}^2(\mu)]^{-d_0/2b_0}, \quad (3.31)$$

has been determined for $N_f = 0$ [12]. We recall that $b_0 = (11 - \frac{2}{3}N_f)/(4\pi)^2$ and $d_0 = 8/(4\pi)^2$ are the lowest order perturbative coefficients of the renormalization group functions for gauge group SU(3). The running mass $\overline{m}(\mu)$ coincides with m_R at some scale $\mu = \mu_0$ and is otherwise determined by the RG equations. The RGI quark mass is non-perturbatively defined, it is scheme and scale independent and hence a natural candidate for a fundamental parameter of QCD. However, it is still customary to quote quark masses in the $\overline{\text{MS}}$ scheme of dimensional regularization at some reference scale. Once M is given, the ratio $\overline{m}^{\overline{\text{MS}}}(\mu)/M$ can be computed by using the perturbative renormalization group functions, which are known with 4-loop accuracy [37,38].

3.3 $O(a)$ improvement

In practice, cutoff effects with Wilson quarks can be rather large, and it is advisable to cancel at least the leading $O(a)$ artefacts in physical observables. One may distinguish cutoff effects which arise already in the chiral limit and those proportional to the quark masses. To cancel the former, a single counterterm, the so-called Sheikholeslami-Wohlert term [39], must be included in the action, with a coefficient c_{sw} which is a function of the bare coupling only. For the improvement of on-shell correlation function one also needs to improve the operators. In our context, only the improvement of the axial current is relevant,

$$(A_I)_\mu = A_\mu + c_A a \tilde{d}_\mu P, \quad (3.32)$$

with the improvement coefficient c_A . Both coefficients are known non-perturbatively for $N_f = 0$ and bare couplings $g_0^2 = 6/\beta \leq 1$ [40].

$O(a)$ artefacts which are proportional to the quark mass m_q can be dealt with perturbatively, as long as am_q is small enough. In practice this may still be the case for the strange quark, but in the case of charm the bare quark mass in lattice units is typically in the range 0.25 – 0.5. In the quenched approximation, the improvement coefficients needed to compute $O(a)$ improved renormalized quark masses are all known non-perturbatively. Renormalization and $O(a)$ improvement of the subtracted bare quark mass is achieved separately for each quark flavour through

$$m_R = Z_m m_q (1 + b_m am_q). \quad (3.33)$$

As for the PCAC quark mass, we first recall the form of the renormalized $O(a)$ improved axial density and current,

$$(A_R)_\mu = Z_A \left[1 + b_A \frac{1}{2} (am_{q,i} + am_{q,j}) \right] (A_I)_\mu, \quad (3.34)$$

$$P_R = Z_P \left[1 + b_P \frac{1}{2} (am_{q,i} + am_{q,j}) \right] P. \quad (3.35)$$

For the quark mass improvement this means

$$m_{R,i} + m_{R,j} = 2Z_A Z_P^{-1} \left[1 + (b_A - b_P) \frac{1}{2} (am_{q,i} + am_{q,j}) \right] m_{ij}. \quad (3.36)$$

Here, it is implicitly assumed that the bare mass m_{ij} is defined including the counterterm $\propto c_A$, i.e.

$$m_{ij} = \frac{\tilde{\partial}_0 f_A(x_0) + c_A a \partial_0^* \partial_0 f_P(x_0)}{2f_P(x_0)}. \quad (3.37)$$

Besides this definition with standard lattice derivatives we also use improved derivatives as in ref. [14]. While the difference is formally an effect of $O(a^2)$ it may be important numerically.

The improvement coefficients b_m and $b_A - b_P$ have been determined for $N_f = 0$ in the relevant range of bare couplings [14]. This, together with the renormalization constants Z [14], Z_A [41] and Z_P [12] allows us to define the renormalized $O(a)$ improved charm quark mass in the SF scheme in various ways. One may then convert from the SF scheme to the RGI quark mass, using the flavour independent ratio $M/\overline{m}(\mu_0)$ in the continuum limit [12]. It is convenient to combine the factors relating the bare current quark mass and the RGI masses into a single one,

$$Z_M = \frac{M}{\overline{m}(\mu_0)} Z_A Z_P^{-1}, \quad (3.38)$$

which has been parameterized in [12] over some range of bare couplings. Up to $O(a^2)$ we then have

$$M_i = Z_M [1 + (b_A - b_P) a m_{q,i}] m_i = Z_M Z m_{q,i} (1 + b_m a m_{q,i}), \quad (3.39)$$

and an analogous equation for $M_i + M_j$ in the mass non-degenerate case.

4 Numerical simulations

The numerical simulations were carried out on machines of the APE100 and APE1000 series using single precision arithmetic and standard algorithms (see ref. [40] for a detailed description and references). Autocorrelation times were found to be small so that our measurements could be treated as statistically independent for all observables considered.

4.1 Simulation parameters

Our choice of simulation parameters is displayed in table 1. The non-perturbatively determined coefficients c_{sw} and c_A were taken from ref. [40]. We chose the same four values of β as in [13], which correspond lattice spacings in the range $a = 0.05 - 0.1$ fm. The conversion to physical units is done using the scale $r_0 = 0.5$ fm [28] and the parameterization of ref. [29],

$$\ln(a/r_0) = -1.6805 - 1.7139(\beta - 6) + 0.8155(\beta - 6)^2 - 0.6667(\beta - 6)^3. \quad (4.40)$$

The lattice size L/a varied between 16 and 32, such that the linear extent of the spatial volume was around $L \simeq 1.5$ fm or larger. For spatial volumes of this size we do not expect any sizeable finite volume effects on our pseudoscalar and vector masses. This is supported by previous findings e.g. in ref. [13], where the pseudoscalar meson mass was found to be safe against finite volume effects, provided its Compton wave length was about 5 times smaller than L . Similar statements are expected to hold for the vector mesons. In the time direction the lattice size varied between 40 and 80, such that the physical extent T/r_0 was kept constant to a good approximation.

β	T/a	L/a	L/r_0	T/r_0	r_0/a	N_{meas}
6.0	40	16	2.98(1)	7.45(3)	5.368(22)	350
6.1	48	24	3.80(2)	7.59(3)	6.324(28)	94
6.2	54	24	3.26(2)	7.34(4)	7.360(35)	159
6.45	80	32	3.06(2)	7.65(4)	10.458(58)	123

Table 1: Simulation parameters, lattice sizes and number of independent measurements.

Our estimates of the hopping parameter for the strange quark are based on table 2 of ref. [13] where the quantity

$$[Z_M R/r_0]_{r_0^2 m_{\text{PS}}^2 = 1.5736} = 1.5736 \times r_0(M_s + \hat{M}), \quad (4.41)$$

is quoted for each value of β . In order to isolate the strange quark mass we use the mass ratio from chiral perturbation theory (2.4). Then we relate the RGI strange quark mass to the subtracted bare quark mass in lattice units,

$$r_0 M_s = (r_0/a) Z_M Z a m_{\text{q,s}} (1 + b_m a m_{\text{q,s}}). \quad (4.42)$$

where we use the coefficients Z and b_m of ref. [14]. Finally, to relate to the corresponding hopping parameter κ_s (3.27), we use estimates of κ_{critical} at $\beta = 6.0, 6.2$ [40], and interpolations at $\beta = 6.1, 6.45$ [42] (cf. table 3). In this way the hopping parameter for the strange quark could be fixed prior to the simulations. As usual, there is some uncertainty associated with the choice of κ_{critical} . In order to assess the sensitivity of our observables to the precise choice of the strange quark mass, we also used a second value of κ_s for all but our largest β -value. Finally, we chose 3 κ -values around the expected physical charm quark mass. The numerical values for all simulated hopping parameters are displayed in table 2.

4.2 D -meson masses

From the correlation functions (3.20–3.22) we determined the corresponding effective masses $m_X(x_0)$ in the pseudo-scalar ($X = \text{PS}$) and vector channel ($X = \text{V}$). In addition we

β	κ	am_q	am	am^{imp}
6.0	0.1190	0.5033	0.5129(2)	0.2962(3)
	0.1200	0.4683	0.4736(2)	0.2913(3)
	0.1210	0.4339	0.4357(2)	0.2837(2)
	0.134108	0.0300	0.0304(3)	0.0299(4)
	0.133929	0.0350	0.0353(3)	0.0346(4)
6.1	0.1218	0.4149	0.4425(2)	0.3113(2)
	0.1224	0.3948	0.4197(2)	0.3030(2)
	0.1230	0.3749	0.3974(2)	0.2940(2)
	0.134548	0.0260	0.0317(3)	0.0312(3)
	0.134439	0.0290	0.0348(3)	0.0342(3)
6.2	0.1230	0.3830	0.4072(2)	0.3086(2)
	0.1235	0.3666	0.3888(2)	0.3000(2)
	0.1240	0.3502	0.3706(2)	0.2909(2)
	0.134959	0.0228	0.0254(2)	0.0253(3)
	0.134832	0.0263	0.0291(2)	0.0288(2)
6.45	0.1270	0.2524	0.2646(1)	0.2336(1)
	0.1280	0.2217	0.2323(1)	0.2094(1)
	0.1290	0.1914	0.2006(1)	0.1844(1)
	0.135124	0.0157	0.0166(1)	0.0165(1)

Table 2: Simulated κ -values and corresponding results for the bare subtracted and bare current quark masses from the mass degenerate PCAC relation.

considered the effective mass m_S associated with the ratio $f(x_0) = k_V(x_0)/f_P(x_0)$, which directly yields the mass splitting between the vector and the pseudoscalar channel. For all parameter choices these effective masses exhibit a plateau. Deviations from the plateau value at small x_0 or small $T - x_0$ are expected, due to the contribution of excited states. Furthermore, since the masses in our work are quite large, the correlation functions decay rapidly and one might expect problems with rounding errors at the larger values of x_0 .

4.2.1 Rounding errors

To estimate rounding errors, we varied the precision of the quark propagator computation. In our production runs the Wilson-Dirac equation was solved with a squared

Analysis of rounding errors

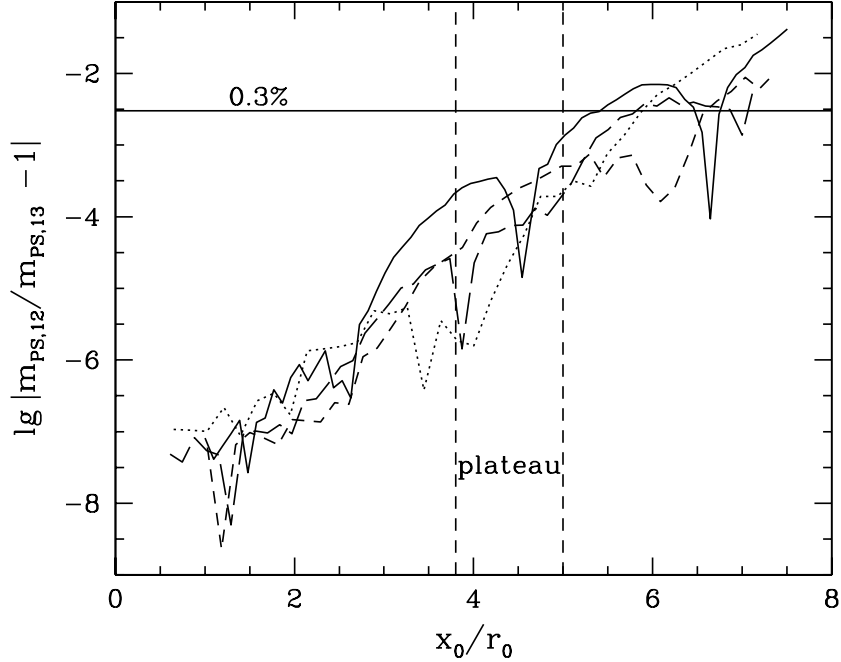


Figure 1: Illustration of the rounding error problem: The plot shows, for all 4 β -values, the logarithm of the relative differences between two effective masses which differ by the solver precision used (cf. text). The curves are obtained as averages over $O(10)$ configurations using the κ_c -value closest to the physical point. The chosen plateau region is indicated by the vertical lines.

relative precision $\epsilon^2 = 10^{-14}$. In addition, at each β value we chose ten independent gauge field configurations, and repeated the calculation with $\epsilon^2 = 10^{-12}$ and $\epsilon^2 = 10^{-13}$. Indicating the solver precision by a superscript, we find that the ratio of effective masses $m_X^{(12)}/m_X^{(13)} - 1$ grows roughly exponentially as a function of the time coordinate. We performed an exponential fit to this ratio of the form $r \exp(x_0 R)$, which was then used to estimate rounding errors on the effective masses. Requiring that the relative error on the masses not exceed a certain value (typically a fraction of a percent) then leads to an upper limit for the range of the plateau. However, note that our method is likely to overestimate this systematic effect, as the limit of single precision is only reached for solver residuals between $\epsilon^2 = 10^{-13}$ and $\epsilon^2 = 10^{-14}$.

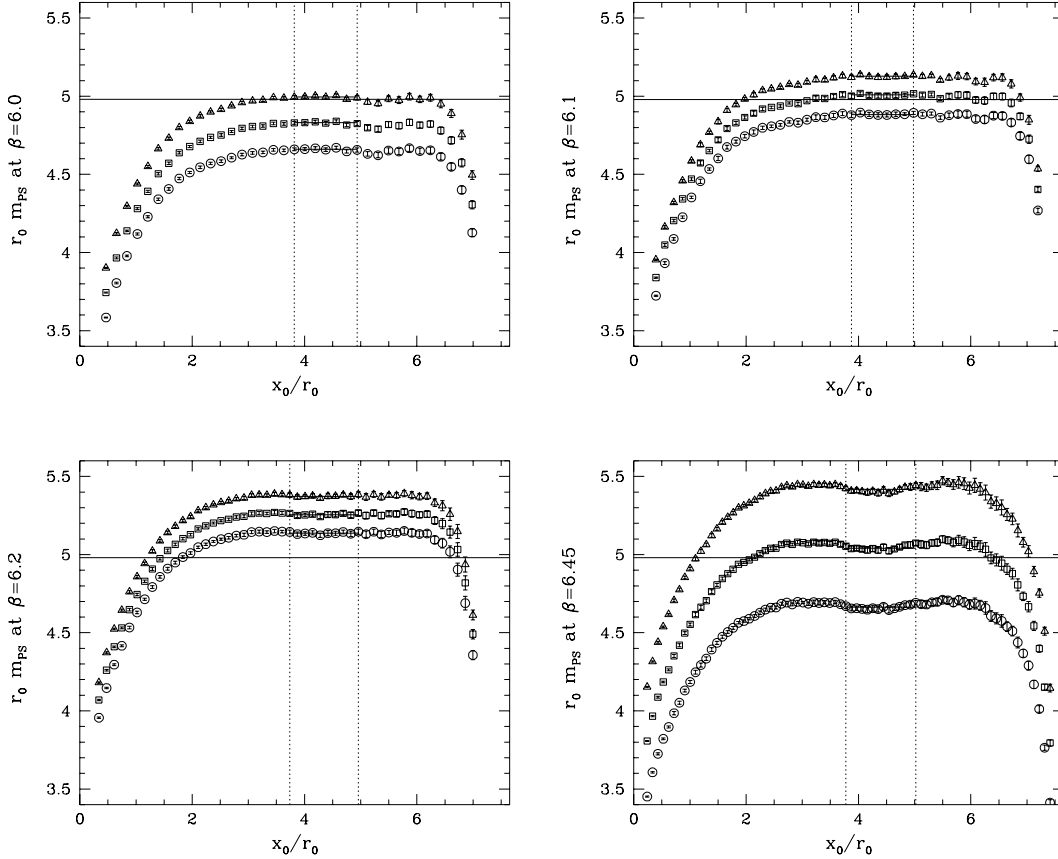


Figure 2: The effective mass plateaux from the correlation function $f_A(x_0)$ for 3 charm quark mass parameters at all β values. The plateaux regions are indicated by the vertical lines. The pseudoscalar meson masses cover the physical D_s meson mass (full line) except at $\beta = 6.2$.

4.2.2 Excited states

To estimate the contributions of excited states to the effective masses we first chose an a priori range for the plateau. Then we averaged $m_X(x_0)$ over the plateau region and subtract the averaged value from $m_X(x_0)$. For small x_0 we fit the remainder with an ansatz of the form $\eta \exp(-x_0 \Delta)$. Reasonable fits could be obtained at all β values, and could be used to quantify the contamination by excited states from the lower time boundary. From the upper boundary at $x_0 = T$ one expects a contribution from the 0^{++} glueball with mass $r_0 m_G \simeq 4.3$ [35]. While in some cases a rough confirmation seemed possible, we essentially assumed this to be the case. In fact, given the problem with rounding errors at large values of x_0 , a clean signal for the glueball state would have come as a surprise.

4.2.3 Plateau regions

Adding all the systematic errors linearly, a plateau region was determined as the interval of times x_0 where the relative systematic error was smaller than some prescribed value. We chose 0.3% for the pseudoscalar mass, 0.5% for the vector mass and 0.8% for the mass splitting. The plateau ranges found in this way were remarkably stable when expressed in physical units. Therefore we decided to define the final ranges as follows: from $3.8r_0$ to $5.0r_0$ for the pseudoscalar masses, from $3.8r_0$ to $5.2r_0$ for the vector masses and from $3.7r_0$ to $4.5r_0$ in the case of the mass splitting. At fixed β and for fixed quark mass parameters, the meson masses are then obtained as averages over the plateau region. Statistical errors were determined by a jackknife procedure, and the maximally allowed systematic error was taken as final systematic error on the effective masses. This is likely to be an overestimate, as the systematic error on the effective masses inside the plateaux is a bit smaller. The results obtained in this way are displayed in table 5.

4.3 Determination of the charm quark mass

The meson masses at the simulated parameter values, can be considered as functions of the corresponding bare valence quark masses. Besides the bare subtracted quark masses (obtained using the κ_{critical} values in table 3), we used bare PCAC masses from the SF correlation functions at $x_0 = T/2$. An analysis of rounding errors for the PCAC masses shows that these are at the level of 0.01% and hence completely negligible. We distinguish the PCAC relation with degenerate and non-degenerate quark masses. Furthermore, we consider two choices of the lattice derivatives used in the PCAC relations: first, the standard choice involving differences between nearest neighbours only, and, secondly, the improved derivatives which also involve next-to-nearest neighbours [cf. [14] for the definitions]. The results are given in tables 2 and 5.

We recall that the strange quark mass parameters were already chosen according to eq. (4.42). Moreover, it turns out that the meson masses only mildly depend on the strange quark mass. Hence it remains to determine the bare charm quark masses where the pseudoscalar meson mass assumes its experimental value,

$$r_0 m_{\text{PS}} = r_0 m_{D_s} = 0.5 \text{ fm} \times 1969 \text{ MeV} = 4.99. \quad (4.43)$$

Our simulation parameters are such that this point could be reached by an interpolation, with the exception of $\beta = 6.2$, where a small extrapolation was required. We performed linear fits of the form

$$r_0 m_{\text{PS}} = \alpha_0 + \alpha_1 r_0 m, \quad (4.44)$$

where m is some definition of the bare charm quark mass. The fits were done inside a Jackknife procedure to take into account correlations of the data points.

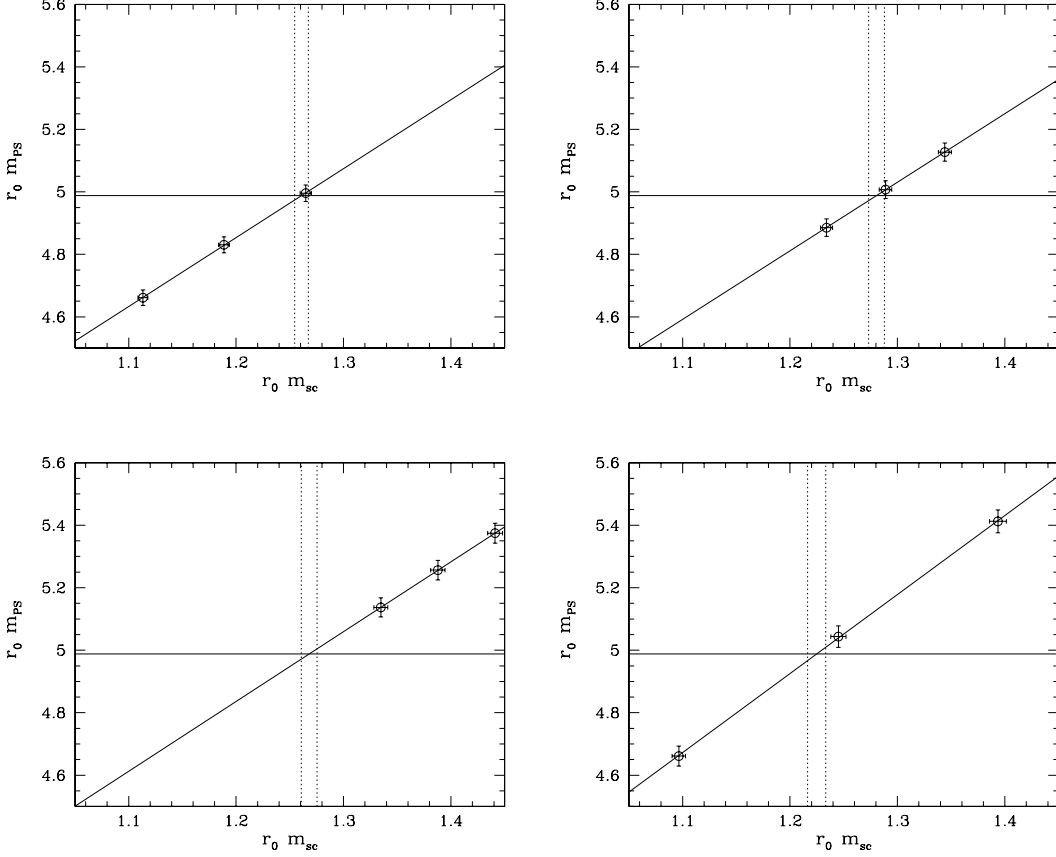


Figure 3: The inter- or extrapolation of m_{PS} as determined from figure 2 vs. the bare charm quark mass $r_0 m_{\text{sc}}$.

Given the various interpolated bare charm quark masses we construct the corresponding $O(a)$ improved RGI masses. We distinguish 5 definitions, the first 3 being given by

$$\begin{aligned}
 r_0 M_{\text{C}}|_{m_{\text{sc}}} &= Z_M \left\{ 2r_0 m_{\text{sc}} \left[1 + (b_A - b_P) \frac{1}{2} (am_{\text{q,c}} + am_{\text{q,s}}) \right] \right. \\
 &\quad \left. - r_0 m_{\text{s}} \left[1 + (b_A - b_P) am_{\text{q,s}} \right] \right\}, \\
 r_0 M_{\text{C}}|_{m_{\text{c}}} &= Z_M r_0 m_{\text{c}} \left[1 + (b_A - b_P) am_{\text{q,c}} \right], \\
 r_0 M_{\text{C}}|_{m_{\text{q,c}}} &= Z_M Z r_0 m_{\text{q,c}} \left[1 + b_{\text{m}} am_{\text{q,c}} \right].
 \end{aligned} \tag{4.45}$$

In addition we use the analogues of the first two definitions but with $m_{\text{sc}} \rightarrow m_{\text{sc}}^{\text{imp}}$ and $m_{\text{c}} \rightarrow m_{\text{c}}^{\text{imp}}$, i.e. using the next-to-nearest derivatives in the PCAC relations. The results are shown in table 4, where the total error is obtained by including the errors of r_0/a , and of the renormalization constants and improvement coefficients in quadrature [cf. table 3].

β	κ_{critical}	Z_M	Z	$b_A - b_P$	b_m
6.0	0.135196	1.752(19)	1.0604(4)	0.171(5)	-0.709(6)
6.1	0.135496	1.782(20)	1.0852(5)	0.071(3)	-0.699(5)
6.2	0.135795	1.807(20)	1.0960(5)	0.039(3)	-0.691(7)
6.45	0.135701	1.852(20)	1.1045(5)	0.010(5)	-0.673(12)

Table 3: Renormalization constants and improvement coefficients at the simulated β -values.

β	$r_0M_c _{m_{sc}}$	$r_0M_c _{m_c}$	$r_0M_c _{m_{q,c}}$	$r_0M_c _{m_{sc}^{\text{im}}}$	$r_0M_c _{m_c^{\text{im}}}$	r_0m_V	r_0m_S
6.0	4.331(59)	5.215(75)	3.224(41)	3.566(47)	3.026(37)	5.281(14)	0.299(11)
6.1	4.274(59)	4.824(70)	3.479(43)	3.755(50)	3.492(44)	5.299(15)	0.303(12)
6.2	4.277(55)	4.682(67)	3.711(47)	3.905(52)	3.769(49)	5.299(15)	0.299(13)
6.45	4.220(60)	4.428(64)	3.975(53)	4.038(57)	3.995(56)	5.300(22)	0.300(17)
<i>CL</i>	4.19(11)	4.20(12)	4.27(10)	4.21(11)	4.31(11)	5.300(35)	0.297(26)

Table 4: Results for the five definitions of the RGI charm quark mass [cf. eqs. (4.45)], the vector meson mass and the mass splitting between vector and pseudoscalar mesons.

5 Continuum extrapolations and results

5.1 RGI charm quark masses

We now come to our main results, the continuum extrapolation of the RGI charm quark mass. As discussed in sect. 3, the charm quark mass can be defined in various ways which are all equivalent up to cutoff effects. Since complete $O(a)$ improvement has been implemented, we attempt linear fits to the data of the form

$$r_0M_c = A + B(a^2/r_0^2), \quad (5.46)$$

with the two parameters A and B . As can be seen in fig. 4, the fits to the data appear very reasonable. Excluding the coarsest lattice spacing, the χ^2 per degree of freedom ranges from 0.1 to 1.5. Moreover, the various definitions of r_0M_c all yield compatible continuum extrapolated results. We also performed combined fits, with the constraint of a common continuum limit. The correlation of the data at the same β -value was taken into account by determining the covariance matrix in a Jackknife procedure. However, the correlation is

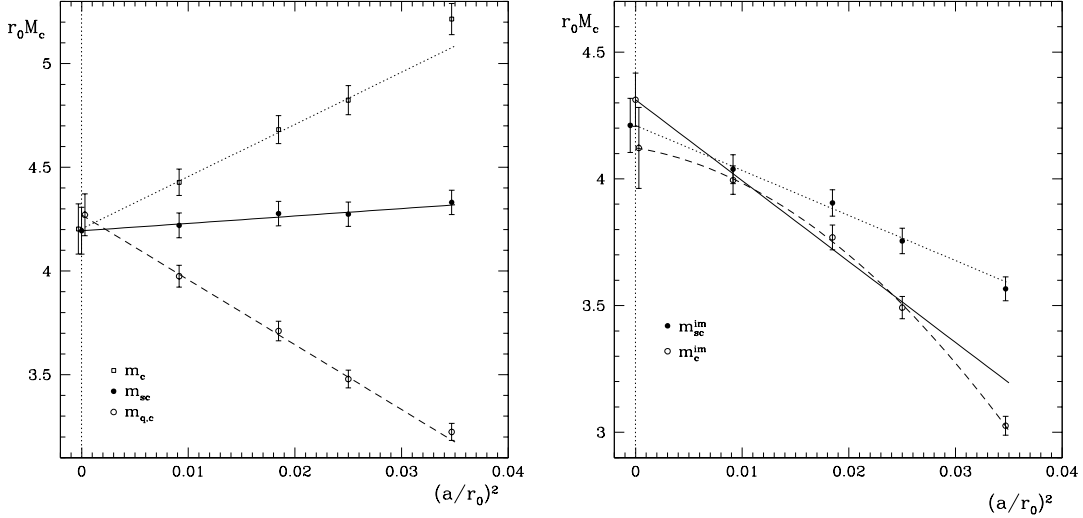


Figure 4: The continuum extrapolation for all 5 definitions of $r_0 M_c$ considered. In the case of $r_0 M_c|_{m_c^{\text{im}}}$ higher order cutoff effects become visible. For illustration we also included a fit to all 4 data points allowing for an additional term $\propto (a/r_0)^4$ (dashed line).

rather strong, so that the error is not much reduced compared to the individual continuum extrapolations.

As our best result we choose the one obtained from the heavy-light PCAC relation, as cutoff effects are found to be rather small in this case. We quote

$$r_0 M_c = 4.19(11), \quad (5.47)$$

where the error contains the 1.3 percent error of the matching factor to the RGI mass [13]. In physical units we then have (with $r_0 = 0.5$ fm)

$$M_c = 1.654(45) \text{ GeV}. \quad (5.48)$$

5.2 Conversion to the $\overline{\text{MS}}$ scheme

In our framework the RGI quark masses appear as the primary quantities. However, many phenomenological applications use the masses in the $\overline{\text{MS}}$ scheme at the scale set by the quark mass itself. In order to convert to this scheme, we integrate the renormalization group equations using the known 4-loop RG functions for $N_f = 0$ [37,38], and find

$$\overline{m}_c^{\overline{\text{MS}}}(\overline{m}_c) = 1.301(28)(20) \text{ GeV} = 1.301(34) \text{ GeV}, \quad (5.49)$$

where we have used the result (2.16) for $\Lambda_{\overline{\text{MS}}}^{(0)}$. The two errors given in the first number correspond to the error in the mass M_c and the change induced by a variation of $\Lambda_{\overline{\text{MS}}}^{(0)}$

within its error bars respectively. As both errors are independent we have combined them quadratically in the last equation of (5.49). Note that the scale of the charm quark mass is already quite low, so that the order of perturbation theory must be specified, too. In fact, using 3 and 2-loop RG evolution we obtain,

$$\overline{m}_c^{\overline{\text{MS}}}(\overline{m}_c) = \begin{cases} 1.294(34) \text{ GeV} & \text{3-loop evolution,} \\ 1.263(34) \text{ GeV} & \text{2-loop evolution,} \end{cases} \quad (5.50)$$

i.e. even the 4-loop contribution is still sizeable, and the difference between 2-loop and 4-loop RG evolution is as large as the total error.

5.3 Further results

5.3.1 The mass ratio M_c/M_s

A further consistency check for our results is provided by considering the ratio M_c/M_s . Here one may compare the continuum extrapolation of the ratio M_c/M_s , to the ratio of the two continuum extrapolated quark masses. Unfortunately, this exercise requires a rather precise tuning of the strange quark mass. As our strange quark mass parameters were tuned using interpolated values of κ_{critical} , the corresponding curve $\kappa_s(\beta)$ does not very precisely correspond to a condition of constant physics. Therefore, instead of using our own data for the strange quark mass, we decided to use the bare current quark masses from ref. [13,42], where a careful extrapolation to the physical kaon mass has been performed. After $\mathcal{O}(a)$ improvement of the bare masses, we take the ratios and combine the errors in quadrature. The continuum extrapolation then yields

$$M_c/M_s = 12.0(5), \quad (5.51)$$

which can be compared to the ratio taken directly in the continuum limit, viz.

$$M_c/M_s = 12.2(1.0). \quad (5.52)$$

5.3.2 $m_{D_s^*}$ and $m_{D_s} - m_{D_s^*}$

We also computed the mass of the vector meson D_s^* . The cutoff effects are very small, so that the continuum extrapolation is not problematic. We obtain

$$r_0 m_{D_s^*} = 5.300(35) \quad \Rightarrow \quad m_{D_s^*} = 2092(14) \text{ MeV}. \quad (5.53)$$

Despite the quenched approximation this is not far from the experimental result, $m_{D_s^*} = 2112 \text{ MeV}$ [2]. It is customary to study the mass splitting $m_S = m_{D_s^*} - m_{D_s}$. Compared to the experimental value of 144 MeV the results of quenched lattice simulations often turn

out to be smaller (see, e.g. [26]). The mass splitting may be obtained in two ways: we may either subtract the input value $r_0 m_{D_s} = 4.99$ from the result (5.53), which yields

$$r_0 m_{D_s^*} - 4.99 = 0.310(35) = 122(14) \text{ MeV} \times 0.5 \text{ fm}. \quad (5.54)$$

On the other hand, the mass splitting may be directly obtained by studying the effective mass associated to the ratio of correlators $f(x_0) = k_V(x_0)/f_P(x_0)$ (cf. sect. 2). With this direct method we obtain in the continuum limit

$$r_0(m_{D_s^*} - m_{D_s}) = 0.297(26) = 117(11) \text{ MeV} \times 0.5 \text{ fm}, \quad (5.55)$$

which agrees with the previous result within errors. Both continuum extrapolations are shown in figure 5, and we conclude that the mass splitting is indeed smaller than the experimental value, albeit only by 1.5 and 2.5 standard deviations for the indirect and direct methods respectively.

5.4 Quenched scale ambiguities

As mentioned in sect. 2, the quenched approximation to QCD accounts for the observed hadronic spectrum up to inconsistencies which are at the 10 per cent level. Turning this around, the choice of different hadronic input from experiment will lead to a spread of results for the Λ parameter and the quark masses in the quenched approximation. Under the assumption that these inconsistencies are entirely due to the neglected sea quark effects, this spread of results may be taken as a first estimate of the quenching error.

We start with some definition of the RGI charm quark mass, consider it as a function of $z = r_0 m_{D_s}$,

$$r_0 M_c = F(z). \quad (5.56)$$

and expand around the standard choice used so far, $z_0 = 4.99$,

$$F(z) = F(z_0) + (z - z_0)F'(z_0) + \text{O}((z - z_0)^2). \quad (5.57)$$

For a 10% shift in the scale r_0 we have $z - z_0 = 0.5$. With this choice we obtain an estimate of the first order term in the continuum limit,

$$0.5F'(4.99) = 0.7(1). \quad (5.58)$$

Expressing M_c again in physical units (using now $r_0 = 0.55 \text{ fm}$!) we observe that the charm quark mass increases by about 6 percent. Although this number is only considered a rough estimate we remark that the approximations made are supported by our data: first, figure 3 indicates that the higher order terms in eq. (5.57) are indeed small over quite some range of charm quark masses. Second, we have assumed that the shift in the strange

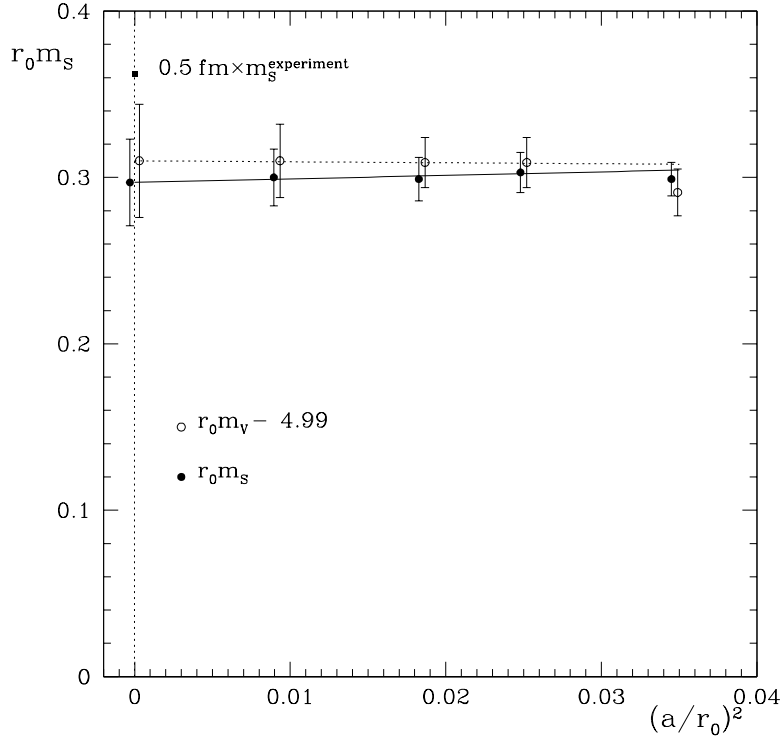


Figure 5: Results for the mass splitting $m_S = m_{D_s^*} - m_{D_s}$. The open points are obtained by computing the vector meson mass while the solid points represent the direct computation of m_S from a ratio of correlation functions (the data points have been slightly offset for clarity).

quark mass can be neglected. As observed in [13], the relative change in the light quark masses is the same as for r_0 itself, due to the proportionality

$$M \propto r_0 m_{\text{PS}}^2. \quad (5.59)$$

As already mentioned earlier the sensitivity of the D_s meson mass to a variation of the strange quark mass is rather low, and this can be seen in table 5, where the differences between the two chosen κ_s -values correspond to 10 – 15 percent differences in the quark mass.

Having established the 6 percent increase of M_c , we note that this corresponds to an increase of only 3 percent for $\overline{m}_c^{\overline{\text{MS}}}(\overline{m}_c)$. This is due to the quark mass anomalous dimension in the $\overline{\text{MS}}$ scheme, which is such that an increase of the renormalization scale decreases the running quark mass. In passing we mention that this also holds for the

strange quark mass at the scale $\mu = 2 \text{ GeV}$ where the induced change amounts to about 8 percent.

The same exercise can be done for the vector meson mass and the mass splitting. The first order terms are now given by

$$0.5F'(4.99) = \begin{cases} 0.46(1) & \text{for } F = r_0 m_{D_s^*}, \\ -0.035(5) & \text{for } F = r_0(m_{D_s^*} - m_{D_s}). \end{cases} \quad (5.60)$$

When expressed in physical units this corresponds to changes of +9% and -20% respectively. Hence, the quenched scale ambiguity for the mass splitting is rather large. In particular, in this latter case the discrepancy to the experimental result increases to about 4 standard deviations.

Finally we look at the ratio M_c/M_s , which may be expected to be less sensitive to the scale ambiguity. Here, the 6% shift of the charm quark mass is overcompensated by the 10% shift in the strange quark mass, leaving a quenched scale ambiguity of about 4%.

5.5 Taking $m_{D_s^*}$ as input

Finally we consider setting the charm quark mass using the D_s^* -meson instead of D_s as input. The analysis is completely analogous and the continuum extrapolations look qualitatively very similar. The D_s mass becomes now a measurement, and the result,

$$r_0 D_s = 5.04(4), \quad (5.61)$$

is not far from the experimental value 4.99 previously used as input. As our best result for the charm quark mass we quote again the value obtained from the mass non-degenerate PCAC mass. The result,

$$r_0 M_c = 4.27(13), \quad (5.62)$$

is slightly larger but consistent within errors with eq. (5.47).

6 Conclusions

The main result of this paper is the determination of the RGI charm quark mass using the experimentally measured D_s meson mass as essential input. Apart from the quenched approximation all errors appear well under control. With specified input the total error is around 3 percent, which is smaller than the error one might attribute to the use of the quenched approximation. An estimate of the latter has been obtained by varying the scale which is used to assign physical units; assuming that the real world is described by full QCD, the inconsistencies may be taken as a first indication of the quenching error. Surprisingly, a scale variation of 10% induces only a 6% shift of the RGI charm quark

mass, which is further reduced to 3% for the charm quark mass in the $\overline{\text{MS}}$ scheme at the charm quark mass scale.

While the agreement with some non-lattice charm quark mass determinations is surprisingly good (in particular the value $\overline{m}_c^{\overline{\text{MS}}}(\overline{m}_c) = 1304(27)$ MeV of ref. [7]) we emphasize that the real quenching error can only be asserted by going beyond the quenched approximation. However, our results show the way towards more realistic studies, as well as the potential strength of lattice techniques. In particular, we draw the following conclusions:

- precise results in charm physics are attainable using the standard set-up of $O(a)$ improved lattice QCD, which was originally designed for the light quarks,
- cutoff effects can be quite large in general, making a continuum extrapolation necessary. In our examples decent continuum extrapolations were possible based on data covering a factor of 2 in the cutoff scale.

Finally, as a by-product of our simulations we measured the D_s^* meson mass and the mass splitting between the vector and pseudoscalar D_s mesons. The latter turns out to be rather small when compared to experiment, and is very sensitive to the quenched scale ambiguity. It will be interesting to look at the effect of sea quarks on the mass splitting.

This work is part of the ALPHA collaboration research programme, and partially supported by the European Community under the grant HPRN-CT-2000-00145 Hadrons/Lattice QCD. Simulations were carried out on machines of the APE100 and APE1000 series at DESY-Zeuthen. We thank the staff at the computer centre for their help, and P. Ball, B. Bunk, T. Hurth, R. Sommer, H. Wittig and U. Wolff for useful discussions.

A Raw lattice data

β	κ_c	κ_s	am_{sc}	am_{sc}^{imp}	am_{PS}	am_{V}	$am_{\text{S}} \times 10^2$
6.0	0.1190	0.134108	0.2356(3)	0.1962(4)	0.9306(16)	0.985(3)	5.55(20)
		0.133929	0.2387(3)	0.1982(4)	0.9366(15)	0.990(3)	5.43(20)
	0.1200	0.134108	0.2214(3)	0.1869(4)	0.8998(16)	0.957(3)	5.80(20)
		0.133929	0.2245(3)	0.1890(3)	0.9058(15)	0.962(3)	5.67(20)
	0.1210	0.134108	0.2074(3)	0.1775(3)	0.8683(15)	0.928(3)	6.06(21)
		0.133929	0.2104(3)	0.1796(4)	0.8744(15)	0.933(3)	5.93(20)
6.1	0.1218	0.134548	0.2125(3)	0.1871(3)	0.811(2)	0.858(3)	4.68(21)
		0.134439	0.2144(3)	0.1885(3)	0.815(2)	0.862(3)	4.64(20)
	0.1224	0.134548	0.2038(3)	0.1806(3)	0.792(2)	0.841(3)	4.81(21)
		0.134439	0.2057(3)	0.1820(3)	0.796(2)	0.844(3)	4.77(20)
	0.1230	0.134548	0.1951(3)	0.1740(3)	0.772(2)	0.823(3)	4.96(21)
		0.134439	0.1970(3)	0.1754(3)	0.776(2)	0.826(3)	4.92(20)
6.2	0.1230	0.134959	0.1958(2)	0.1770(2)	0.730(2)	0.769(3)	3.73(19)
		0.134832	0.1980(2)	0.1787(3)	0.735(1)	0.773(2)	3.67(17)
	0.1235	0.134959	0.1886(2)	0.1713(2)	0.714(2)	0.754(3)	3.84(18)
		0.134832	0.1907(2)	0.1730(2)	0.719(1)	0.758(2)	3.77(17)
	0.1240	0.134959	0.1814(2)	0.1655(3)	0.698(1)	0.739(3)	3.95(19)
		0.134832	0.1835(2)	0.1673(3)	0.703(1)	0.743(2)	3.88(17)
6.45	0.1270	0.135124	0.1332(2)	0.1270(2)	0.518(2)	0.544(3)	2.59(18)
	0.1280		0.1191(2)	0.1142(2)	0.482(1)	0.512(3)	2.82(20)
	0.1290		0.1049(2)	0.1012(2)	0.446(1)	0.478(3)	3.09(20)

Table 5: Results for unrenormalized current quark and meson masses for all heavy-light combinations of simulated κ -values (errors are statistical only).

References

- [1] K. Hagiwara et al. [Particle Data Group Collaboration], Phys. Rev. D **66** (2002) 010001
- [2] D. E. Groom et al. [Particle Data Group Collaboration], Eur. Phys. J. C **15** (2000) 1.
- [3] F. Jegerlehner, arXiv:hep-ph/0105283.
- [4] P. Gambino and M. Misiak, Nucl. Phys. B **611** (2001) 338.
- [5] T. Hurth, in *Proc. of the 5th International Symposium on Radiative Corrections (RADCOR 2000)* ed. Howard E. Haber, arXiv:hep-ph/0106050.
- [6] A. D. Martin, J. Outhwaite and M. G. Ryskin, Eur. Phys. J. C **19** (2001) 681.
- [7] J. H. Kühn and M. Steinhauser, Nucl. Phys. B **619** (2001) 588.
- [8] M. Eidemüller and M. Jamin, Phys. Lett. B **498** (2001) 203.
- [9] S. Narison, Phys. Lett. B **520** (2001) 115.
- [10] J. Penarrocha and K. Schilcher, Phys. Lett. B **515** (2001) 291.
- [11] for a review and further references cf. S. Sint, Nucl. Phys. Proc. Suppl. **94** (2001) 79.
- [12] S. Capitani, M. Lüscher, R. Sommer and H. Wittig [ALPHA Collaboration], Nucl. Phys. B **544** (1999) 669.
- [13] J. Garden, J. Heitger, R. Sommer and H. Wittig [ALPHA Collaboration], Nucl. Phys. B **571** (2000) 237.
- [14] M. Guagnelli, R. Petronzio, J. Rolf, S. Sint, R. Sommer and U. Wolff [ALPHA Collaboration], Nucl. Phys. B **595** (2001) 44.
- [15] T. Bhattacharya, R. Gupta, W. J. Lee and S. R. Sharpe, Phys. Rev. D **63** (2001) 074505.
- [16] C. R. Allton, M. Ciuchini, M. Crisafulli, E. Franco, V. Lubicz and G. Martinelli, Nucl. Phys. B **431** (1994) 667.
- [17] A. Bochkarev and P. de Forcrand, Nucl. Phys. B **477** (1996) 489; Nucl. Phys. Proc. Suppl. **53** (1997) 305.
- [18] A. S. Kronfeld, Nucl. Phys. Proc. Suppl. **63** (1998) 311.

- [19] V. Gimenez, L. Giusti, F. Rapuano and M. Talevi, Nucl. Phys. B **540** (1999) 472.
- [20] D. Becirevic, V. Lubicz and G. Martinelli, Phys. Lett. B **524**, 115 (2002).
- [21] H. Leutwyler, Phys. Lett. B **378** (1996) 313.
- [22] J. Gasser and H. Leutwyler, Annals Phys. **158** (1984) 142.
- [23] J. Bijnens, G. Ecker and J. Gasser, arXiv:hep-ph/9411232.
- [24] M. B. Wise, Phys. Rev. D **45** (1992) 2188.
- [25] G. Burdman and J. F. Donoghue, Phys. Lett. B **280** (1992) 287.
- [26] K. C. Bowler, L. Del Debbio, J. M. Flynn, G. N. Lacagnina, V. I. Lesk, C. M. Maynard and D. G. Richards [UKQCD Collaboration], Nucl. Phys. B **619** (2001) 507.
- [27] A. Duncan, E. Eichten and H. Thacker, Phys. Rev. Lett. **76** (1996) 3894; Phys. Lett. B **409** (1997) 387
- [28] R. Sommer, Nucl. Phys. B **411**, 839 (1994).
- [29] M. Guagnelli, R. Sommer and H. Wittig, Nucl. Phys. B **535** (1998) 389.
- [30] R. G. Edwards, U. M. Heller and T. R. Klassen, Nucl. Phys. B **517** (1998) 377.
- [31] S. Necco and R. Sommer, Nucl. Phys. B **622** (2002) 328.
- [32] M. Lüscher, S. Sint, R. Sommer and P. Weisz, Nucl. Phys. B **478** (1996) 365.
- [33] M. Lüscher, R. Narayanan, P. Weisz and U. Wolff, Nucl. Phys. B **384** (1992) 168.
- [34] S. Sint, Nucl. Phys. B **421** (1994) 135.
- [35] M. Guagnelli, J. Heitger, R. Sommer and H. Wittig [ALPHA Collaboration], Nucl. Phys. B **560** (1999) 465.
- [36] S. Sint and P. Weisz [ALPHA collaboration], Nucl. Phys. B **545** (1999) 529
- [37] T. van Ritbergen, J. A. Vermaseren and S. A. Larin, Phys. Lett. B **400** (1997) 379; **405** (1997) 327;
- [38] K. G. Chetyrkin, Phys. Lett. B **404** (1997) 161.
- [39] B. Sheikholeslami and R. Wohlert, Nucl. Phys. B **259** (1985) 572.
- [40] M. Lüscher, S. Sint, R. Sommer, P. Weisz and U. Wolff, Nucl. Phys. B **491** (1997) 323.

[41] M. Lüscher, S. Sint, R. Sommer and H. Wittig, Nucl. Phys. B **491** (1997) 344.

[42] H. Wittig, private communication.